International Journal of Thales Natural Sciences (IJTNS)
ISSN (online): 2528-9446

Physical Properties of Honeycomb BiTeCl

M. Nurullah Secuk
Yuzuncu Yil University,Van, TURKEY

HarunAkkus
Yuzuncu Yil University,Van, TURKEY

ABSTRACT

From physical properties of double-layer honeycomb BiTeCl crystal electronic, thermodynamic and elastic ones have been investigated using density functional theory under the local density approximation (LDA) in this study. Electronic properties were studied without spin-orbit interaction (SOI) and band gap was found as 1.132 eV which is in good agreement with previous theoretical studies without SOI, but different from experimental ones. Ground state properties of new type ferroelectric BiTeCl such as lattice parameters, electronic total density of states (TDOS), partial density of states (PDOS) and electronic band structure, change of Helmholtz free energy, internal energy, entropy and constant volume specific heat by increasing temperature, elastic stiffness and compliance constants, stability conditions and related elastic properties were studied in detail.

Keywords: Hexagonal, density functional theory, electronic, thermodynamic, elastic

1 INTRODUCTION

Theoretical and experimental investigations on structural, elastic, electronic, optic, dynamic and thermodynamical properties of crystals are highly attractive areas of research [1-9]. Since ferroelectric materials can show dielectric, piezoelectric and pyroelectric properties, a wide industrial area of application exists for them. Especially ferroelectric semiconductors can be used in sound convertors, sonar detectors, memory materials, etc [10, 17]. First invented ferroelectric is $BaTiO_3$, and then highly sensitive fotoconducting material SbSI group of $A^{V}B^{VI}C^{VII}$ semiconductors were found [18]. The search for more efficient, cheaper, multi-functional materials has increased interest for new types of ferroelectrics [19-26]. In this context, from $A^{V}B^{VI}C^{VII}$ type new ferroelectric semiconductors bismuth tellurohalids (BiTeCl, BiTeBr, BiTeI) are important materials in that they can be used in spintronics due to Rashba split, as memory materials and also they show topological insulating properties (insulating in bulk region but conducting at surface), different surfaces can behave as different type (n or p) of semiconductors [27, 28].

So we investigated structural properties of double-layer honeycomb BiTeCl crystal using density functional theory under the generalized gradient (GGA) and the local density approximations. The best convergence was gathered by LDA and electronic, thermodynamic and elastic calculations were fulfilled only under LDA.

From X-ray powder diffraction [29] it was determined that crystal structure of BiTeCl is hexagonal of space group $P6_3mc$ (186) and point group 6mm with lattice parameters of a= 8.107 and c=23.426 Bohr, z=2, unit cell volume of V_0= 1304.091 $(Bohr)^3$ and the crystal structural is given in Figure 1. In this study

structural optimization of BiTeCl was performed in four steps as written below and optimization results were given in Table 1:

- Total energy optimization with respect to cutoff kinetic energy of plane waves (up to 52 Ha) (E_{cut}-E_{tot}opt.).
- Total energy optimization with respect to number of k points up to 24x24x24 grid (ngkpt-E_{tot} opt.).
- Atomic optimization (with 5 % dilation) for lattice parameters, volume of unit cell and reduced coordinates (At. opt.).
- Volume optimization of 60 steps for lattice parameters and unit cell volume by reduced coordinates found in atomic optimization step (Vol. opt. by at. opt. xred).

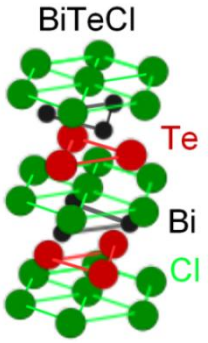

Figure 1: Crystal structure of double layer bismuth tellurochloride [30].

Table 1 Results of four step optimization for bismuth tellurochloride

Property	**E_{cut}-E_{tot} opt.**	**ngkpt-E_{tot} opt.**	**At. opt.**	**Vol. opt. by at. opt. xred**	**Exp.**
E_{cut}	40 Ha	-	-	-	-
ngkpt (nkpt)	-	14x14x14 (168)	-	-	-
a (Bohr)	-	-	7.757	7.723	8.017
c (Bohr)	-	-	22.471	23.133	23.426
V_0 $(Bohr)^3$	-	-	1170.956	1195.014	1304.091

Nearest calculated value of volume to the experimental one is of the step of volume optimization by reduced coordinates found in atomic optimization. Thus, for the rest of calculations lattice parameters and reduced coordinates were taken from this step of optimization.

2 COMPUTATIONAL METHOD

Electronic, thermodynamic and elastic properties of new type ferroelectric BiTeCl was investigated using ABINIT [31] under density functional theory. Calculations belonging to structural optimization were fulfilled by both GGA and LDA and best results were gathered within LDA by the FHI98PP self-consistent pseudopotentials [32] with the Ceperley-Alder-Perdew-Wang scheme that takes into account the exchange-correlation effects [33, 34]. Thus, main topics of this article were studied only under LDA.

For solving Kohn-Sham equations the conjugate gradient minimization method [35] was chosen [36]. Plane augmented waves were used as basis set for electronic wave functions. LDA based pseudopotentials accept true valance electrons as $6s^26p^3$ for Bi, $5s^25p^4$ for Te and $3s^23p^5$ for Cl. Structural optimizations were done to a good convergence at 40 Ha of cutoff energy and 168 k points using

14x14x14Monkhorst-Pack mesh grid [37] in BiTeCl crystal, but for best results higher values of cutoff energy and mesh grids were utilized in the calculations of electronic and elastic properties.

3 ELECTRONIC PROPERTIES

For electronic structure calculations of bismuth tellurochloride without SOI, pseudopotential method was used within LDA based on density functional theory (DFT). In fact, a grid of 14x14x14 was enough but for best accuracy we have chosen it as 24x24x24 in spite of consuming more time and producing 1872 k points which is far above the required number. As can be seen in partial and total density of states (PDOS and TDOS) in Figure 2, main contribution to valance band comes from 5p orbital of Te and 6p orbital of Bi atoms.

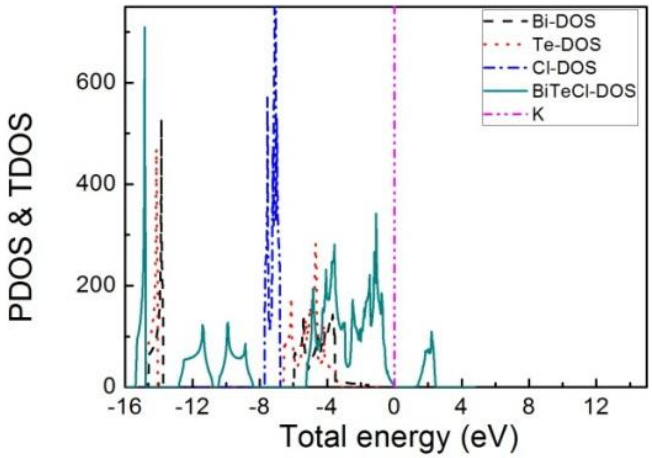

Figure 2: PDOS' and TDOS for BiTeCl with Fermi energy level adjusted to 0 eV.

Calculated electronic band structure and TDOS for BiTeCl are given in Figure 3 where Fermi energy level (E_F) is adjusted to 0 eV. Band gap can be obviously seen in both of band energy diagram and DOS just above E_F.

BiTeCl crystal has 18 valence bands and additional 18 conduction bands were used for band structure calculations. According to band structure calculations, in which Fermi level was set to zero, BiTeCl crystal has a direct band gap, as can be seen in figure 3, at Γ high symmetry point with a value of 1.132 eV that is near to those calculations done without SOI [38]. Band gaps for all high symmetry points are given in Table 2.

Some of existing experimental and theoretical results on band gap of BiTeCl are given in table 3. The difference between experimental results and calculated ones originates from two main factors as utilizing pseudopotential method and ignoring SOI. Pseudopotential method and inherent intractability of density functional theory can cause different estimations of band gaps up to 50 % error, mostly underestimated [39], but sometimes overestimated band gaps can be gathered in calculations [38]. Overestimation in band gap is attributed to the nature of pseudopotentials used and large spin orbit coupling (SOC) effect of Bi atom [41], which causes Rashba splitting in real crystal and band gap decreases.

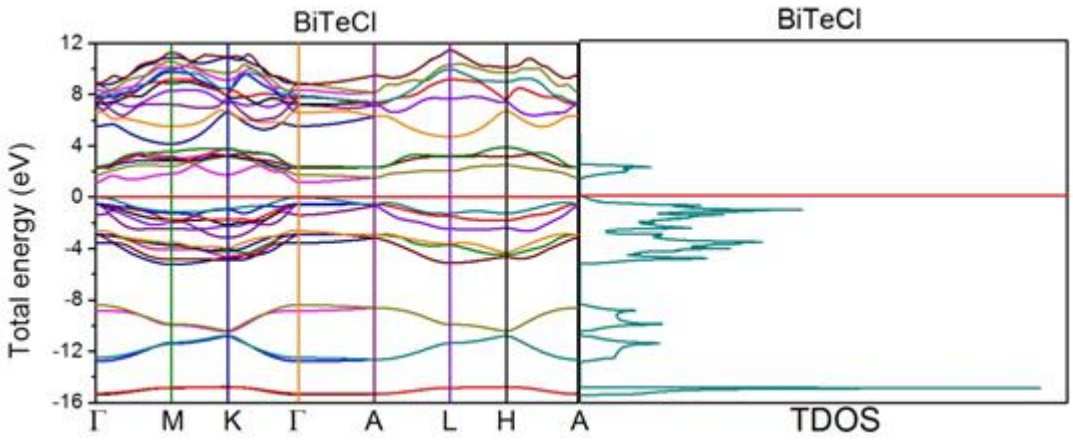

Figure 3: Electronic band structure and DOS for BiTeCl with E_F adjusted to 0 eV

Table 2Band gaps (in eV) at high symmetry points of BiTeCl in matrix form

	Γ	M	K	A	L	H
Γ	**1.132**	1.812	1.699	1.585	1.925	2.491
M	.	2.944	2.831	2.718	3.057	3.624
K	.	.	2.604	2.491	2.831	3.397
A	.	.	.	2.038	2.378	2.944
L	.	.	.	.	3.171	3.737
H	.	.	.	.	.	3.737

Table 3Theoretical and experimental results on band gap of BiTeCl in eV

Ref. [30] (Exp.)	Ref. [40] (Exp.)	Ref. [38] (Theo.)	Ref. [41] (Theo.)	Ref. [41] (Theo.with SOI)	Present work(Theo)
0.77	0.7	1.2	~1.2	~0.7	1.132

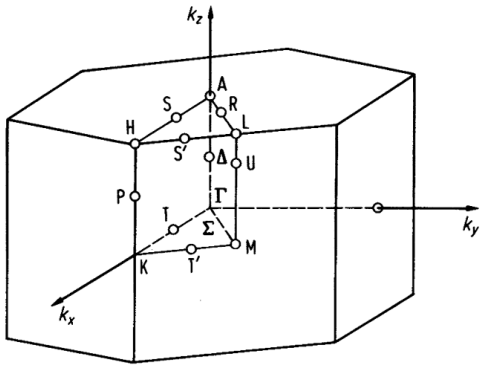

Figure 4: High symmetry points and paths in first Brillouin zone in reciprocal space for hexagonal bismuth tellurochloride[42].

From Figure 4 it is seen that high symmetry points of Γ and A are on the path of Δ, parallel to k_Z axis in first Brillouin zone of hexagonal structure, the path Γ-A is highly degenerate and band structure is non-parabolic, its dependence to k is nearly linear with a very low slope. Band structure is mostly non-degenerate in the path of Γ-M-K-Γ. Also, band structure is approximately independent of k at all symmetry points.

4 THERMODYNAMICPROPERTIES

Thermodynamical properties of BiTeCl crystal were calculated using phonon band structure calculations by 50 Ha cutoff energy (although 40 was enough) and 6x6x6 grids with 28 q points [43]. The entropy (S), the constant-volume specific heat (C_V), phonon contributions to Helmholtz free energy (F) and internal energy (E) as a function of temperature for BiTeCl crystal are given in Figure 5a and Figure 5b. The contributions of phonons, i.e. of lattice, to internal and free energies do not vanish at zero temperature. The contributions of phonons to Helmholtz free energy, F_0, and internal energy, E_0, are same and equal to 11300 J/mol at zero Kelvin, as in Figure 5a, which shows that zero-point oscillations exist. As temperature increases, internal energy also increases as expected, but Helmholtz free energy decreases because F is not only a function of E, but it depends on temperature also by equation (1):

$$F = E - TS \tag{1}$$

Entropy increases with increasing temperature, as it should be, and a linear increase is seen especially above 250 K in Figure 5b.

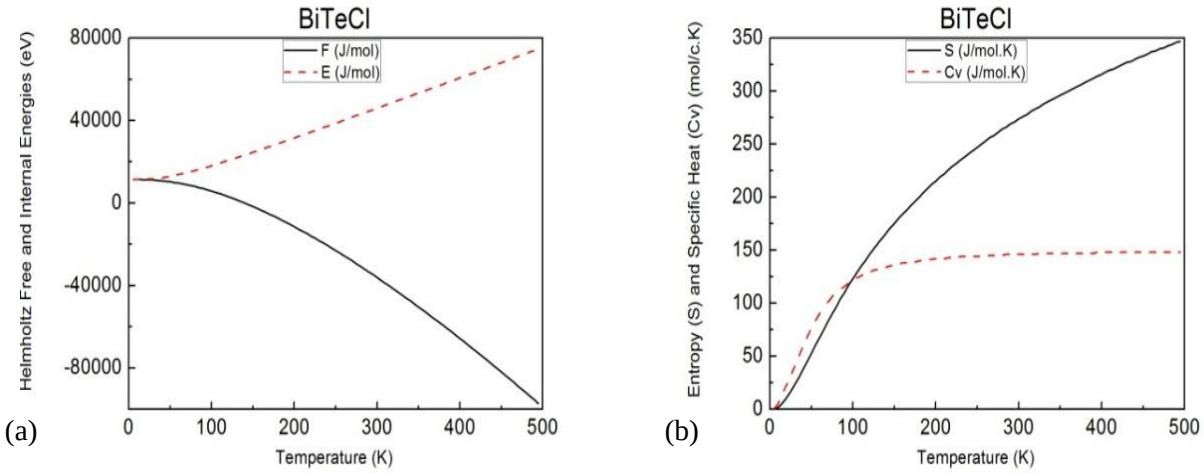

Figure 5: a) Helmholtz free (F) and internal energies (E), b) entropy (S) and constant-volume specific heat (C_V) for BiTeCl

Constant-volume specific heat for BiTeCl crystal was found from phonon calculations and it approaches a limit value of 147.81 J/mol.K at about 400 K, which is very close to the value of 149.66 J/mol.K as seen in Figure 5b, the classical Dulong-Petit limit [44] of specific heat that is expressed as C_v=3nR where R= 8.3145 J/mol.K and number of atoms in primitive cell of BiTeCl (n) is 6. At low temperatures, especially below 20 K, far below Debye temperature Θ_D, T^3 law overwhelms which is expressed as in (2):

$$C_V = \frac{12\pi^4}{5} N_A k_B \left(\frac{T}{\theta_D}\right)^3 \tag{2}$$

where N_A is Avagadro's number and k_B is Boltzmann's constant. At low temperatures quantum effects of material becomes important in contributing C_V. Since our crystal is a semiconductor, free electrons do not exist and so, not only at low, but at any temperature a significant contribution of electrons to specific heat does not occur.

5 ELASTICPROPERTIES

Many fundamental features of crystals are closely related to elastic properties, that means they depend on elastic constants. Some of these elastic constant dependent features are inter-atomic and intra-molecular bonding, intrinsic (microscopic) hardness, macroscopic hardness, microcracks, machinability, structural stability, specific heat, melting temperature, thermal expansion, equation of state and especially for superconductors Debye temperature, electron-phonon coupling constant and critical temperature [45-48].

For high accuracy in calculations of elastic constants, mesh grids of 14x14x14, 16x16x16 and 18x18x18, strain of 5 %, ionmov of 2 (for both conserving symmetry and keeping volume constant) and ecut of 50 Ha were used and average of results of different mesh grids were accepted as elastic constants of BiTeCl crystal.

The relationship between stress (σ_{ij}) applied on a material and strain (ε_{ij}) formed in the tensor form are:

$$\sigma_{ij} = c_{ijkl}\varepsilon_{kl} \tag{3}$$

$$\varepsilon_{ij} = s_{ijkl}\sigma_{kl} \tag{4}$$

whereσ_{ij} are coefficients of stress tensor while ε_{kl} are of the strain tensor, c_{ijkl} and s_{ijkl} are the stiffness compliance tensors which are reciprocal of one another.

Elastic stiffness constants, C_{ij}, and elastic compliance constants, S_{ij}, of any crystal are expressed by 6x6 symmetric matrices. In fact, C_{ij}, is reduced form of symmetric stiffness tensor of c_{ijkl} of rank 4 and it has 81 elements. By symmetry and index reductions of 11=1, 22=2, 33=3, 23=32=4, 31=13=5 and 12=21=6, number of elements of elastic constant tensor is reduced to 36. Number of independent elements of the matrix depends on crystal class. After index reduction elastic stress and strain are found as below:

$$\sigma_i = \sum_{i=1}^{6} C_{ij}\varepsilon_j \tag{5}$$

$$\varepsilon_i = \sum_{i=1}^{6} S_{ij}\sigma_j \tag{6}$$

There are only 2 independent elastic constants (C_{11} and C_{12}) of isotropic materials, but for cubic ones 3, for hexagonals 5, for tetragonal-I and rhombohedral-I groups 6, for tetragonal-II and rhombohedral-II groups 7, in orthorhombic crystals 9, for monoclinic ones 13 and for the most anisotropic group of crystals -triclinics- 21 independent elastic constants exist. 5 independent elastic constants of hexagonal crystals are C_{11}, C_{12}, C_{13}, C_{33} and C_{44}. In calculations we find C_{66} also, but it is not independent, it is C_{66}=(C_{11}-C_{12})/2 [49, 50]. From diagonal elements C_{11} andC_{33} are constants about compression (bulk), while C_{44} is of shear. Elastic matrix for hexagonal crystals is as in below:

$$C_{ij}=\begin{pmatrix} C_{11} & C_{12} & C_{13} & 0 & 0 & 0 \\ \cdot & C_{11} & C_{13} & 0 & 0 & 0 \\ \cdot & \cdot & C_{33} & 0 & 0 & 0 \\ 0 & 0 & 0 & C_{44} & 0 & 0 \\ 0 & 0 & 0 & 0 & C_{44} & 0 \\ 0 & 0 & 0 & 0 & 0 & C_{66} \end{pmatrix}=\begin{pmatrix} C_{11} & C_{12} & C_{13} & & & \\ \cdot & C_{11} & C_{13} & & & \\ \cdot & \cdot & C_{33} & & & \\ & & & C_{44} & & \\ & & & & C_{44} & \\ & & & & & C_{66} \end{pmatrix}$$

A general method to check whether calculated elastic constants are appropriate numbers for stable physical structure or not, there is a procedure and the following conditions should be provided for any crystal to be able stable [50]:

- Det $[C_{ij}] > 0$, where i, j= 1, 2, … 6.
- Det $[U^{ij}] > 0$, where U^{ij} is upper-left sub-matrices of C_{ij}.
- All $\lambda_i > 0$, where λ_i are eigenvalues of C_{ij} and i= 1, 2 … 6.
- All $C_{ii} > 0$, where C_{ii}'s are diagonal elements of C_{ij} and i, j= 1, 2, … 6.

When these steps were performed, one can find the following three ***required and sufficient*** conditions of stability, which are called as Born-Huang stability conditions for hexagonal crystals [49, 50]:

- $C_{11} - |C_{12}| > 0$
- $C_{44} > 0$
- $C_{33}(C_{11}+C_{12})-2C_{13}^{2} > 0$

One can find compliance constants, S_{ij}, by using determinant and sub-determinants of C_{ij}as following [51]:

$$S_{ij}=\frac{(-1)^{i+j}\det(U_{ij})}{\det(C_{ij})} \qquad (7)$$

whereU_{ij} is sub-matrix of C_{ij}up to the C_{ij}. This is compliance tensor for hexagonal crystal:

$$S_{ij}=\begin{pmatrix} S_{11} & S_{12} & S_{13} & 0 & 0 & 0 \\ \cdot & S_{11} & S_{13} & 0 & 0 & 0 \\ \cdot & \cdot & S_{33} & 0 & 0 & 0 \\ 0 & 0 & 0 & S_{44} & 0 & 0 \\ 0 & 0 & 0 & 0 & S_{44} & 0 \\ 0 & 0 & 0 & 0 & 0 & S_{66} \end{pmatrix}=\begin{pmatrix} S_{11} & S_{12} & S_{13} & & & \\ \cdot & S_{11} & S_{13} & & & \\ \cdot & \cdot & S_{33} & & & \\ & & & S_{44} & & \\ & & & & S_{44} & \\ & & & & & S_{66} \end{pmatrix}$$

Explicit conversions [51, 52] between stiffness (C_{ij}) and compliance (S_{ij}) constants can be derived using (7) as in the following equations:

$$C_{11}=\frac{S_{11}S_{33}-S_{13}^{2}}{\det(S_{ij})}=\frac{S_{33}}{2S}+\frac{1}{2(S_{11}-S_{12})} \qquad C_{12}=\frac{S_{13}^{2}-S_{12}S_{33}}{\det(S_{ij})}=\frac{S_{33}}{2S}-\frac{1}{2(S_{11}-S_{12})}$$

$$C_{13} = \frac{S_{12}S_{13} - S_{11}S_{13}}{\det(S_{ij})} = -\frac{S_{13}}{S} \qquad C_{33} = \frac{S_{11}^2 - S_{12}^2}{\det(S_{ij})} = \frac{S_{11} + S_{12}}{S}$$

$$C_{44} = \frac{1}{S_{44}} \quad C_{66} = \frac{1}{S_{66}} \text{ where} \qquad S = S_{33}(S_{11} + S_{12}) - 2S_{13}^2 \tag{8}$$

Any one of two methods above can be chosen to find out C_{ij}'s from S_{ij}'s.Also, one can have compliance constants S_{ij}'s by existing stiffness constants C_{ij}'s just by replacing C by S and S by C.

Table 4 Calculated stiffness (GPa) and compliance (GPa^{-1}) constants with data from literature

C_{ij}	Present work (LDA)	Literature (GGA) [38]	S_{ij}	Present work (LDA)	By the data of literature (GGA) [38]
C_{11}	78.37	56.6	S_{11}	0.04038	0.03037
C_{12}	37.92	20.8	S_{12}	0.01565	0.00243
C_{13}	52.37	47.6	S_{13}	-0.05265	-0.01616
C_{33}	55.73	96.6	S_{33}	0.11691	0.02628
C_{44}	33.71	1.7	S_{44}	0.02966	0.58824
C_{66}	20.22	17.9	S_{66}	0.04945	0.05587

Elastic constants of BiTeCl are given in table 4 and they provide all of general [50] and special (***required and sufficient***) [49, 50] conditions of stability, so BiTeCl is a mechanically stable crystal. The value of C_{11} is greater than that of C_{33}, which means that crystal is stiffer against compressions along "a" axis while softer and thus more compressible along "c" axis. That means bonds among nearest neighbors along "c" axis (along {001} planes) are weaker than that along "a" axis (along {100} planes). C_{44} shows the shear along 23 (i.e. yz) plane, that is along (100) planes as parallel to "c" axis of hexagonal crystal. C_{66} shows the shear along 12 (i.e. xy) plane, that is along (001) planes as parallel to base of crystal. Since C_{44} is greater than C_{66}, one can infer that reaction to plastic deformation (i.e. shear) along (100) plane is more than the shear along (001) plane which makes it easier to deform BiTeCl along (001) (i.e. xy) plane, parallel to base of hexagon, as perpendicular to "c" axis rather than along (100) (i.e. yz) plane, parallel to "c" axis, as perpendicular to base of hexagon. Table 5 is about calculated mass, volume and density of BiTeCl.

Table 5 Calculated mass, volume and density of BiTeCl primitive cell.

Property	Symbol	Present work (LDA)	Literature (GGA) [38]	Unit
Mass	M_0	$1.24.10^{-24}$	-	kg
Volume	V_0	$1.93.10^{-28}$	-	m^3
Density	ρ	$6.39.10^3$	$6.41.10^3$	kg/m^3

Source of differences in density and density-related calculations is that since volume is underestimated by LDA and overestimated by GGA, density found by LDA is less than that found by GGA.

A comprehensive list of elastic properties of BiTeCl, their symbols and units are given in the table 6 with the lone result in the literature. The ways to calculate elastic properties by using 5 independent elastic constants for all hexagonal crystals are given in the Appendix.

Table 6 Calculated and literature data of elastic properties for BiTeCl

	Property	**Symbol and Unit**	**Present work (LDA)**	**Literature (GGA) [38]**
1.	Voight Bulk Modulus	B_V (GPa)	55.31	49.1
	Reuss Bulk Modulus	B_R (GPa)	54.49	36.8
	Hill Bulk Modulus	B_H (GPa)	54.90	42.9
2.	Voight Shear Modulus	G_V (GPa)	22.18	10.5
	Reuss Shear Modulus	G_R (GPa)	10.17	3.6
	Hill Shear Modulus	G_H (GPa)	16.17	7.0
3.	Young Modulus	E (GPa)	44.18	20.0
4.	Poisson Ratio	ν (-)	0.37	0.42
5.	Lame Constant -1	μ (GPa)	16.17	-
6.	Lame Constant -2	λ (GPa)	44.12	-
7.	Pugh Indicator (K= B/G)	K (-)	3.39	6.10
8.	Machinability Index	μ_M (-)	1.63	-
9.	Longitudinal Sound Speed	v_l(m/s)	3458.3	2856.0
10.	Transverse Sound Speed	v_t(m/s)	1590.5	1047.4
11.	Average Sound Speed	v_m(m/s)	1792.1	1189.2
12.	Debye Temperature	Θ_D (K)	116.3	111.4
13.	ZenerAnisotropy Index	A (-)	1.67	-
14.	Universal Anisotropy Index	A^U (-)	5.93	10.1
15.	Bulk Anisotropy Percentage	A_B (-)	0.74	14.37
16.	Shear Anisotropy Percentage	A_G (-)	37.15	49.40
17.	Equivalent Zener Anisotropy Index	A^{eq}(-)	6.79	-
18.	Shear Anisotropy Index for {100} Planes Between [011] and [010] Directions	A_1 (-)	4.59	-
19.	Shear Anisotropy Index for {010} Planes Between [101] and [001] Directions	A_2 (-)	4.59	-
20.	Shear Anisotropy Index for {001} Planes Between [110] and [010] Directions	A_3 (-)	1.00	-
21.	Bulk Modulus Along Axis “a”	B_a (GPa)	296.42	-
22.	Bulk Modulus Along Axis “b”	B_b (GPa)	296.42	-
23.	Bulk Modulus Along Axis “c”	B_c(GPa)	86.18	-
24.	Relaxed Bulk Modulus	B_{relax}(GPa)	54.49	-

25.	Unrelaxed Bulk Modulus	$B_{unrelax}$(GPa)	55.31	-
26.	Anisotropy Index of Bulk Modulus Along Axis "a" with respect to Axis "b"	A_{Ba}(-)	1.00	-
27.	Anisotropy Index of Bulk Modulus Along Axis "c" with respect to Axis "b"	A_{Bc}(-)	0.29	-
28.	Minimum Thermal Conductivity	$K_{min}(Wm^{-1}K^{-1})$	0.906	0.273
29.	Shear Wave Modulus	C_s (GPa)	20.22	-
30.	Kleinman Coefficient	ξ (-)	0.61	-
31.	Lineer Compressibility Coefficient	$f=k_c/k_a$(-)	3.44	-
32.	Average Compressibility Coefficient	β (GPa^{-1})	0.02	-

Bulk modulus (B) is reaction of material against compressibility, fracture, while shear modulus (G) is a measure of reaction of crystal to plastic deformation [54]. Bulk modulus is related to average bond strength and shear modulus is about resistance for changing angle of bond [49]. Voight value is upper bound for a modulus, it corresponds to equating strain throughout crystalline body to a uniform external strain (ε_i= *Constant*), it is measured under external pressure and in this case bulk modulus is equal to $B_{unrelax}$. Reussvalue is lower bound for a modulus, it corresponds to equating stress throughout crystalline body to a uniform external stress (σ_i= *Constant*), it is measured without external pressure (or under hydrostatic pressure which is equal at every point of crystalline structure making the pressure difference zero for any two points in the body of the crystal) and in this case bulk modulus equals to B_{relax}[55] as can be seen in the table 6 where for our case B_V and $B_{unrelax}$ values show 55.31 GPa while values of B_R and B_{relax} are the same and equal to 54.49 GPa. For both of bulk and shear moduli, Hill value is used as average of upper (Voight) and lower (Reuss) values because Voight and Reuss values are correct only for isotropic materials, for those with anisotropy average (Hill) value should be utilized. Young modulus is a measure of stiffness for materials and the more the Young modulus the more the stiffness. Calculated Young modulus shows that BiTeCl is as hard as most of metals and it is relatively soft for shear.

Lame constant 1 (μ) physically represents the compressibility of a crystal, while Lame constant 2 (λ) shows shear stiffness of the material. Values of μ and λ show that the crystal is relatively compressible and soft.

Bulk modulus is much bigger than shear, thus for stability of BiTeCl crystal the limiting parameter is shear modulus. Pugh indicator (K= B/G) was found as 3.39 which shows that material is of ductile nature because the values above 1.75 are accepted as ductility region whereas below that is the region of brittileness. Thus, we can conclude that material is malleable. For ionic materials B/G ratio is about 0.9 while for covalent materials this ratio is about 1.6 [54]. Here, B/G ratio is 3.39 which implies that metallic contribution to bonding overwhelms because metallic Bi and semi-metallic Te atoms have intra-layer [38] and interlayer metallic bonds, even if inter-layer covalent bonds exist between Te and Cl slabs, and even if Bi and Te can make coordinate covalent bonds with Cl. In any case, B/G ratio shows that metallic bonds are prevalent in this crystal. A calculated value of 1.63 for machinability is also indicator of ductile nature of BiTeCl.

Poisson ratio is an indicator of bonding type, stiffness in crystals and it is a measure of stability of crystal [55] against shear [56]. Poisson ratio takes values in the interval of 0-0.5 and small ratios show relative stability against shear [55], while large values indicate less stability. Forces in the crystal are of non-central type if Poisson ratio is less than 0.25. For crystals of which bonds are of covalent character Poisson ratio is about 0.1, for ionic character bonds it takes usually the value of 0.25 and for metallic ones takes values between 0.25 and 0.45; in our case with a value of 0.37 for σ, metallic bond character appears again [38] with forces of rather central character. Ratios of C_{13}/C_{44} and C_{12}/C_{66} are 1.58 and 1.88 which are not too far from unity that also shows rather centrality of forces.

Using sound waves in different directions one can calculate elastic constants of a crystal experimentally. If elastic constants are once found, we can find out longitudinal, transverse and average sound waves in crystal by formulae given in Appendix. By using average sound wave, one can calculate Debye temperature which is an important parameter of solid because it relates elastic constants and many physical properties of a solid, such as specific heat, melting temperature, vibrational entropy, etc. Values of Debye temperatures calculated in this study and given in literature are 116.3 K and 111.4 K, respectively.

Anisotropy can be correlated with microcracks and different nature of bonds along different directions in the crystal [47]. For an isotropic crystal elastic anisotropy (A and A^{eq}) is equal to 1 and deviations from 1 show anisotropic nature of material [57]. In case of universal anisotropy index (A^{U}) a value of zero means isotropy and higher values show anisotropy. Moreover, bulk (compressibility) (A_B) and shear (A_G) anisotropic percentagesare 0 for isotropic case, while departures from zero means anisotropy and maximum value of anisotropy can be 1 (i.e. 100%). Almost all of anisotropy measures show that BiTeCl is an anisotropic material except A_B, which implies that material is nearly isotropic against compression, and A_3 that means crystal is isotropic in terms of shear for {001} planes between [110] and [010] directions. Elastic anisotropy of BiTeCl single crystal arises from different natures of bonds intra-slabs metallic bonds within distinct Bi and Te slabs and inter-slabs Te-Cl covalent bonds. Shear anisotropies of A_1 and A_2 are equal because lattice parameters of a and b in hexagonal structure are equal.

Thermal conductivity shows heat transfer rate of a material and especially for crystals it indicates that either the crystal can be used as heat barrier or not. For our case minimum thermal conductivity was calculated as 0.906 which is far from another theoretical calculation [38], but in both calculations it is seen that thermal conductivity of BiTeCl is near to common insulators.

Value of linear compressibility coefficient (f) is 3.44 which shows that BiTeCl crystal is less compressible along {100} planes (i.e. parallel to of "c" axis and perpendicular to the base of crystal) than along {001} planes (i.e. parallel to base of crystal and perpendicular to "c" axis). This should be originated from difference in bond strengths between inter-slabs and intra-slabs. Intra-slab bonds are stronger than inter-layer ones. This implies that BiTeCl is relatively softer in "c" direction and stiffer in "a" axis. That is, reactions against compressibility (bulk modulus) along "a" and "b" axes (which are equal in hexagonal crystals) should be much more than that along "c" axis which is proven by values of B_a= B_b=296.42 GPa and B_c=86.18 GPa values. Small (0.29) value of anisotropy index of bulk modulus along axis "c" with respect to axis "b" (A_{Bc}) also indicates that fact. Value of average compressibility was calculated as 0.02 which originates from large difference between values of B and G.

Shear wave module C_s given here is calculated for cubics but in case of hexagonal symmetry it corresponds to shear component of C_{66}. UnitlessKleinman coefficient ξ is an internal strain parameter for cubics and it is about relative positions of cations and anions for the case of strains where the symmetry of crystal is conserved but atomic positions not. For hexagonal BiTeCl it was calculated as 0.61.

6 CONCLUSION

From electronic properties total and partial DOS', band structure, from thermodynamic features F, E, S, C_V and from elastic properties elastic stiffness and compliance constants, stability conditions and several related important elastic properties were studied in detail. Result of band gap is in coherence with theoretical studies without SOI and different from experimental values, calculated thermodynamic features are found as expected, and some of elastic properties could be compared with existing theoretical data but no comparison with experimental results could be done for elastic features due to the lack of experimental studies.

7 ACKNOWLEDGEMENTS

The calculations reported in this paper were partially done at TUBITAK ULAKBIM, High Performance and Grid Computing Center (TRUBA resources) and Theoretical Physics Lab. of Physics Department at YuzuncuYil University.

APPENDIX

Required formulas for calculating some of elastic properties by using elastic constants are given in the list below.

1. Bulk Modulus (B) (*GPa*) [49]
   $B_V= (2C_{11}+2C_{12}+4C_{13}+C_{33})/9$
   $B_R= \{(C_{11}+C_{12})C_{33}-2C_{13}^2\}/(C_{11}+C_{12}+2C_{33}-4C_{13}) = C^2/M$ or
   $B_R= 1/[(S_{11}+S_{22}+S_{33})+2(S_{12}+S_{13}+S_{23})]$
   $B=B_H= (B_V+B_R)/2$
2. Shear Modulus (G) (*GPa*) [49]
   $G_V= (C_{11}+C_{12}+2C_{33}-4C_{13}+12C_{44}+12C_{66})/30$ or
   $G_V= 15/[4(S_{11}+S_{22}+S_{33})- 4(S_{12}+S_{13}+S_{23}) + 3(S_{44}+S_{55}+S_{66})]$
   $G_R= \{[(C_{11}+C_{12})C_{33}-2C_{13}^2]C_{44}C_{66}\}/\{3B_VC_{44}C_{66}+[(C_{11}+C_{12})C_{33}-2C_{13}^2](C_{44}+C_{66})\}5/2$
   $G=G_H= (G_V+G_R)/2$
3. Young Modulus (E) (*GPa*) [49, 59]
   $E= 9B_HG_H/(3B_H+G_H)$
4. Poisson Ratio (v) (-)[49]
   $v= (3B_H-2G_H)/[2(3B_H+G_H)]$
5. Lame Constant-1 (μ) (*GPa*) [58]
   $\mu= E/[2(1+v)]$
6. Lame Constant-2 (λ) (*GPa*) [58]
   $\lambda= vE/[(1+v)(1-2v)]$
7. Pugh Indicator (K) (-) [47, 49, 55, 58, 59]
   $K= B/G$
8. Machinability Index (μ_M) (-) [48, 60]
   $\mu_M= B_H/C_{44}$
9. Longitudinal Sound Speed (v_l) (*m/s*) [40, 47, 56, 59, 60]
   $v_l= [(B+4G/3)/d]^{1/2}$
10. Transverse Sound Speed (v_t) (*m/s*) [40, 47, 50, 59, 60]
    $v_t= (G/d)^{1/2}$
11. Average Sound Speed (v_m) (*m/s*) [40, 47, 50, 59, 60]
    $v_m= [(v_l^{-3}+2v_t^{-3})/3]^{-1/3}$
12. Debye Temperature (Θ_D) (K) [40, 47, 50, 59]
    $\Theta_D= [h/(2\pi k_B)](6\pi^2nN_Ad/M)^{1/3}v_m$
13. Zener Anisotropy Index (A) [57, 59]
    $A= 2C_{44}/(C_{11}-C_{12})= C_{44}/C_{66}$
14. Universal Anisotropy Percentage (A^U) (-) [40, 47, 57, 59]
    $A^U= 5G_V/G_R+B_V/B_R-6$
15. Bulk Anisotropy Percentage (A_B) (-) [40, 47]
    $A_B = 100(B_V-B_R)/(B_V+B_R)$

16. Shear Anisotropy Index (A_G) (-)[40, 47]
$A_G = 100(G_V-G_R)/(G_V+G_R)$

17. Equivalent Zener Anisotropy Index (A^{eq}) [57]
$A^{eq} = (1+5A^U/12)+ \{(1+5A^U/12)^2-1\}^{1/2}$

18. Shear Anisotropy Index for {100} Planes Between [011] and [010] Directions (A_1) (-)
$A_1= 4C_{44}/(C_{11}+C_{33}-2C_{13})$ [40, 47]

19. Shear Anisotropy Index for {010} Planes Between [101] and [001] Directions (A_2) (-)
$A_2= 4C_{55}/(C_{22}+C_{33}-2C_{23})$ [40, 47]
$A_2= 4C_{55}/(C_{11}+C_{33}-2C_{13})$

20. Shear Anisotropy Index for {001} Planes Between [110] and [010] Directions (A_3) (-)
$A_3= 4C_{66}/(C_{11}+C_{22}-2C_{12})$ [40, 47]
$A_3= 4C_{66}/(C_{11}+C_{11}-2C_{12})= 4C_{66}/(2C_{11}-2C_{12})= 2C_{66}/(C_{11}-C_{12})= C_{66}/[(C_{11}-C_{12})/2]C_{66}/C_{66}=1$

(For hegxagonal structrures only $\alpha=1$, but for cubics $\alpha=1$, $\beta=1$) [40]
$\alpha=[(C_{11}-C_{12})(C_{33}-C_{13})-(C_{23}-C_{13})(C_{11}-C_{13})] / [(C_{33}-C_{13})(C_{22}-C_{12})-(C_{13}-C_{23})(C_{12}-C_{23})]$
$\alpha=[(C_{11}-C_{12})(C_{33}-C_{13})-(C_{13}-C_{13})(C_{11}-C_{13})] / [(C_{33}-C_{13})(C_{11}-C_{12})-(C_{13}-C_{13})(C_{12}-C_{13})]$
$\alpha=[(C_{11}-C_{12})(C_{11}-C_{12})-0] / [(C_{11}-C_{12})(C_{11}-C_{12})-0]= 1$

$\beta=[(C_{22}-C_{12})(C_{11}-C_{13})-(C_{11}-C_{12})(C_{23}-C_{12})] / [(C_{22}-C_{12})(C_{33}-C_{13})-(C_{12}-C_{23})(C_{13}-C_{23})]$ [40]
$\beta=[(C_{11}-C_{12})(C_{11}-C_{13})-(C_{11}-C_{12})(C_{13}-C_{12})] / [(C_{11}-C_{12})(C_{33}-C_{13})-(C_{12}-C_{13})(C_{13}-C_{13})]$
$\beta=[(C_{11}-C_{12})\{(C_{11}-C_{13})-(C_{13}-C_{12})\}] / [(C_{11}-C_{12})(C_{33}-C_{13})]$
$\beta=\{(C_{11}-C_{13})-(C_{13}-C_{12})\}/(C_{33}-C_{13})$
$\beta=\{(C_{11}+C_{12}-2C_{13})\}/(C_{33}-C_{13})= f$

$\Lambda= C_{11}+ C_{22}\alpha^2+C_{33}\beta^2+2C_{12}\alpha+2C_{13}\beta +2C_{23}\alpha\beta$ [40]
$\Lambda= C_{11}+ C_{11}\alpha^2+C_{33}\beta^2+2C_{12}\alpha+2C_{13}\beta +2C_{13}\alpha\beta$
$\Lambda= C_{11}+ C_{11}.1^2+C_{33}\beta^2+2C_{12}.1+2C_{13}\beta +2C_{13}.1\beta$
$\Lambda= 2C_{11}+2C_{12}+C_{33}\beta^2+4C_{13}\beta$

$\Lambda_{(\alpha=\beta=1)}= 2C_{11}+2C_{12}+C_{33}+4C_{13}$ [40]

21. Bulk Modulus Along Axis "a" (B_a) (*GPa*) [40]
$B_a = a(dP/da)=\Lambda/(1+\alpha+\beta)=\Lambda/(1+1+\beta)=\Lambda/(2+\beta)$

22. Bulk Modulus Along Axis "b" (B_b) (*GPa*) [40]
$B_b = b(dP/db)= B_a/\alpha= B_a/1= B_a$

23. Bulk Modulus Along Axis "c" (B_c) (*GPa*) [40]
$B_c = c(dP/dc)= B_a/\beta$

24. Relaxed Bulk Modulus (B_{relax}) (*GPa*) [40]
$B_{relax}=\Lambda/(1+\alpha+\beta)^2=\Lambda/(1+1+\beta)^2=\Lambda/(2+\beta)^2$

25. Unrelaxed Bulk Modulus ($B_{unrelax}$) (*GPa*) [40]
$B_{unrelax,(\alpha=\beta=1)}= \Lambda_{(\alpha=\beta=1)}/(1+\alpha+\beta)^2= \Lambda_{(\alpha=\beta=1)}/(1+1+1)^2= \Lambda_{(\alpha=\beta=1)}/9$

26. Anisotropy Index of Bulk Modulus Along Axis "a" with respect to Axis "b" (A_{Ba}) (-)
$A_{Ba} = B_a/B_b=\alpha=1$ [40]

27. Anisotropy Index of Bulk Modulus Along Axis "c" with respect to Axis "b" (A_{Bc}) (-)

$A_{Bc} = B_c/B_b = \alpha/\beta = 1/\beta$ [40]

28. Minimum Thermal Conductivity (K_{min}) (-) [38]
$K_{min} = k_B n^{2/3}(2v_t + v_l)$

29. Shear Wave Modulus (C_s) (*GPa*) [56]
$C_s = (C_{11}-C_{12})/2 = C_{66}$

30. Kleinman Coefficient (ξ) (-) [56]
$\xi = (C_{11}+8C_{12})/(7C_{11}+2C_{12})$

31. Lineer Compressibility Coefficient ($f=k_c/k_a$) (-) [48, 60]
$f = (C_{11}+C_{12}-2C_{13})/(C_{33}-C_{13})$

32. Average Compressibility Coefficient (β) (1/*GPa*) [48, 58, 60]
$\beta = 1/B_H$

REFERENCES

[1] Alward J.F., Fong C.Y., El-Batanouny M. and Wooten F.(1978). Electronic and optical properties of SbSBr. SbSI and SbSeI Solid State Com., 25, 307.

[2] Edwardson P.J., Boyer L.L., Newman R.L., Fox D.H., Hardy J.R., Flocken J.W., Guenther R.A. and Mei W.(1989). Ferroelectricity in perovskitelike $NaCaF_3$ predicted ab initio. Phys. Rev. B, 39, 9738.

[3] Akkus H. and Erdinc B.(2009) First-principles study of $NaCdF_3$. Phys. Status Solidi B, 246, 1334.

[4] Flocken J.W., Guenther R.A., Hardyand J.R. and Boyer L.L.(1985). First-principles study of structural instabilities in halide-based perovskites: Competition between ferroelectricity and ferroelasticity. Phys. Rev. B, 31, 7252.

[5] Bingol S., Erdinc B. and Akkus H.(2015). Electronic band structure, optical, dynamical and thermodynamic properties of cesium chloride (CsCl) from first-principles. International Journal for Simulation and Multidisciplinary Design Optimization (IJSMDO), 6, A7.

[6] Gulebaglan S.E.(2012).The bowing parameters of $Ca_\chi Mg_{1-\chi}O$ ternary alloys. Modern Physics Letters B, 26, 1250199–8.

[7] Erdinc B., Soyalp F. and Akkus H.(2011). First-principles investigation of structural, electronic, optical and dynamical properties in CsAu. Cent. Eur. J. Phys., 9, (5) 1315-20.

[8] Erdinc B., Akkus H. and Goksen K.(2010). Electronic and optical properties of GaS: A firstprinciples study. Gazi University Journal of Science (GU J Sci), 23(4), 413–22.

[9] Erdinc B., Aycibin M., Secuk M.N., Gulebaglan S.E., Doğan E.K. and Akkus H.(2014). Theoretical Study of Rhombohedral $NaCaF_3$ Crystal in the predicted ferroelectric phase. Gazi University Journal of Science GU J Sci), 27(4), 1093–97.

[10] AkkusH. and Mamedov A.(2006). Ab-initio calculation of band structure and linear optical properties of SbSI in para- and ferroelectric phases. Open Physics, 5(1), 25–34.

[11] Akkus H., Kazempour A., Akbarzadeh H. and Mamedov A.M.(2007). Band structure and optical properties of SbSeI: density-functional calculation. Physica Status Solidi B, 244 (10), 3673–83.

[12] Akkus H., MamedovA., KazempourA. and AkbarzadehH.(2008). Band structure and optical properties of antimony-sulfobromide: density functional calculation. Open Physics, 6(1), 64–75.

[13] Koc H., Akkus H. and Mamedov A.M.(2012). Band structure and optical properties of BiOCl: Density functional calculation. Gazi University Journal of Science (GU J Sci), 25(1), 9–17.

[14] Akkus H., Cabuk S. and Mamedov A.M.(2010).Linear and nonlinear optical susceptibilities in some ferroelectrics: Ab-initio calculation.Int. J. Nanoelectronics and Materials, 3, 53–67.

[15] Akkus H.(2009).Density functional calculation of the electronic structures of some $A^5B^6C^7$-type crystals. International Journal of Modern Physics B, 23(1), 97–104.

[16] Scott J.F., Araujo C.A. and Mcmillan L.D.(1989). "Ferroelectric Memory Applications IEEE 1989 Ultrasonics Symposium," Proceedings Vols 1 and 2, pp. 299–308.

[17] Uchino K. Ferroelectirc Devices.(2000). (New York: Marcel Dekker Inc.)

[18] Fatuzzo E., Harbeke G., Merz W.J, Nitsche R., Roetschi H. and Ruppel W. (1962). Ferroelectricity in SbSI.Phys. Rev., 127, 2036.

[19] Duran D., Erdinc B., Aycibin M. and AkkusH.(2015). Linear optical properties of ferroelectric semiconductor Bi_2NbO_5F crystal. Ferroelectrics, 486, 25–32.

[20] Ota Y., Abe T. and Inushima T.(2011).Phonon frequencies of ferroelectric semiconductor SbSBr by first principle calculation. Ferroelectrics, 414, 113.

[21] Audzijonis A., Zigas L. and Kvedaravicius A.(2012).The nature of anharmonicity and anomalous piezoelectric properties of ferroelectric SbSBr crystal. Physica B, 407, 774.

[22] Akkus H. and Mamedov A.M.(2007).Linear and nonlinear optical properties of SbSI: First-principle calculation. Ferroelectrics, 352, 148.

[23] Li J.F., Viehland D., Bhalla A. and Cross L.E.(1992).Pyro-optic studies for infrared imaging. J. App. Phys., 71, 2106.

[24] Akkus H. and Mamedov A.M.(2007).Ab initio calculations of the electronic structure and linear optical properties, including self-energy effects, for paraelectric SbSI. J. Phys. Condens. Matter, 19, 116207.

[25] Audzijonis A and Sereika R 2010 The thermodynamic functions of SbSBr crystal Phase Trans. 83 389

[26] Dogan E.K., Aycibin M., Gulebaglan S.E., Secuk M.N., Erdinc B. and Akkus H.(2013).Structural, thermodynamic and phonon properties of SbSI and SbSBr single crystals.Journal of the Korean Physical Society, 63, 2133–37.

[27] Sakano M. et al.(2013). Strongly spin-orbit coupled two-dimensional electron gas emerging near the surface of polar semiconductors. Phys. Rev. Lett., 110, 107204.

[28] Zhiyong Z., Cheng Y. and Schwingenschlög U.(2013). Orbital-dependent Rashba coupling in bulk BiTeCl and BiTeI. New Journal of Physics, 15, 023010.

[29] Shevelkov A.V., Dikarev E.V., Shpanchenko R.V. and Popovkin B.A.(1995).Crystal structures of bismuth tellurohalides BiTeX (X = Cl, Br, I) from X-Ray Powder Diffraction Data. J. of Sol. Stat.Chem., 114, 379–84.

[30] Akrap A., Teyssier J., Magrez A., Bugnon P., Berger H., Kuzmenko A.B., Marel van der D. (2014).Optical properties of BiTeBr and BiTeCl. Phys. Rev. B, 90, 035201.

[31] Gonze X. et al.(2002). First-principles computation of material properties: the ABINIT software project. Comput. Mat. Sci., 25, 478.

[32] Fuch M. and Scheffler M.(1999).Ab initio pseudopotentials for electronic structure calculations of poly-atomic systems using density functional theory. Comput. Phys. Commun., 119, 67-98.

[33] Perdew J.P. and Wang Y.(1992).Accurate and simple analytic representation of the electron-gas correlation energy. Phys. Rev. B, 45, 13244.

[34] Perdew J.P., Burke K. and Ernzerhof M.(1996). Generalized gradient approximation made simple. Phys. Rev. Lett., 77, 3865.

[35] Payne M.C., Teter M.P., Allan D.C., Arias T.A. and Joannopoulos J.D.(1992). Iterative minimization techniques for ab initio total-energy calculations: molecular dynamics and conjugate gradients. Rev. Mod. Phys., 64, 1045.

[36] Kohn W. and Sham L.J.(1965).Self-consistent equations including exchange and correlation effects. Phys. Rev., 140, A1133.

[37] Monkhorst H.J. and Pack J.D.(1976). Special points for Brillouin-zone integrations. Phys. Rev. B, 13, 5188.

[38] Zhou S., Long J. and Huang W.(2014). Theoretical prediction of the fundamental properties of ternary bismuth tellurohalides. Materials Science in Semiconductor Processing, 27, 605–10.

[39] Wang Z.M.(2014). MoS_2: Materials, Physics, and Devices, Lecture Notes in Nanoscale and Technology, 21, 58.

[40] Jacimovic J. et al.(2014).Enhanced low-temperature thermoelectrical properties of BiTeCl grown by topotactic method. Scripta Materialia, 76, 69.

[41] ZhiyongZ., Yingchun C. and Schwingenschlögl U.(2013).Orbital-dependent Rashba coupling in bulk BiTeCl and BiTeI. New Journal of Physics, 15, 023010.

[42] http://exciting-code.org/forum/t-222178/k-space-high-symmetry-points

[43] Secuk M.N., Akkus H., Erdinc B., Gulebaglan S.E.,Aycibin M. and DoganE.K.(2015). Structural, dynamic and optical properties of double-layer hexagonal BiTeCl Crystal. International Conference on Pure and Applied Mathematics (ICPAM 2015), 1, 200.(Van/Turkey/http://icpam.yyu.edu.tr/Abstract%20Book.pdf)

[44] Secuk M.N., Aycibin M., Erdinc B., Gulebaglan S.E., DoganE.K. and Akkus H.(2014).Ab-initio calculations of structural, electronic, optical, dynamic and thermodynamic properties of HgTe and HgSe. American Journal of Condensed Matter Physics, 4(1), 13–19.

[45] Shein I.R. and Ivanovskii A.L.(2011). Elastic properties and inter-atomic bonding in new superconductor KFe2Se2 from first principles calculations.

http://arxiv.org/ftp/arxiv/papers/1102/1102.3248.pdf

[46] Hirsch J.E.(1997). Correlations between normal-state properties and superconductivity. Phys. Rev. B, 55, 9007.

[47] Shein I.R. and Ivanovskii A.L.(2011).Elastic properties of superconducting MAX phases from first-principles calculations.Physica Status Solidi B,248(1), 228–32.

[48] Bannikov V.V., Shein I.R. and Ivanovskii A.L.(2011). Elastic and electronic properties of hexagonal rhenium sub-nitrides Re3N and Re2N in comparison with hcp-Re and wurtzite-like rhenium mononitrideReN. Phys. Status Solidi B, 248 (6), 1369–74

[49] Wu Z., Zhao Er-jun, Xiang Hong-ping, Hao Xian-feng, Liu Xiao-juan and JianMeng.(2007).Crystal structures and elastic properties of superhard IrN2and IrN3 from first principles. Phys. Rev. B, 76, 054115.

[50] Mouhat F. and Coudert F.X.(2014).Necessary and sufficient elastic stability conditions in various crystal systems. Phys. Rev. B, 90, 224104.

[51] Green D.J.An Introduction to the Mechanical Properties of Ceramics,(1998),pp. 325.

[52] Nye J.F.Physical Properties of Crystals.(1976), pp. 147.

[53] Shein I.R. and Ivanovskii A.L.(2011).Elastic properties and inter-atomic bonding in new superconductor KFe_2Se_2 from first principles calculations.Solid State Communications, 151 (9), 67–73.

[54] Ravindran P., Fast L., Korzhavyi P.A. and Johansson B.(1998).Density functional theory for calculation of elastic properties of orthorhombic crystals: application to $TiSi_2$. J. Appl. Phys., 84, 4891.

[55] Hou H.J., Kong F.J., Yang J.W., Wan S.Q. and Yang S.X.(2013).Ab-initio calculations of physical properties of alkali chloride XCl (X = K, Rb and Li) under pressure.Physica B, 428, 5-9.

[56] Ranganathan S.I. and Ostoja-Starzewski M.(2008). Universal elastic anisotropy index. P.R.L., 101, 055504.

[57] Qi-Jun L., Ning-Chao Z., Fu-Sheng L. and Zheng-Tang L.(2014). Structural, electronic, optical, elastic properties and Born effective charges of monoclinic HfO_2 from first-principles calculations. Chin. Phys. B, 23 (4), 047101.

[58] Wang P., Z Jiang-yi, Zhang X-dong and Lin Y-ming.(2015).A first principles study of orthorhombic $Ca(BH_4)_2$. Science Journal of Northwest University Online, 13, (1).

[59] Nan-Xi M., Chun-Ying P., Chao-Zheng H, Fei-Wu Z., Cheng L., Zhi-Wen L. and Da-Wei Z.(2014). Mechanical and thermodynamic properties of the monoclinic and orthorhombic phases of SiC_2N_4 under high pressure from first principles. Phys. B, 23 (12), 127101.

[60] Zhang X., Ying C., Ma H., Shi G. and Li Z.(2013). First principles study on lattice dynamics, thermodynamics and elastic properties of Na_2Te under high pressure. Phys. Scr., 88, 035602.